**Structural Engineering and Mechanics**, *Vol. 57, No. 3 (2016) 441-456*
DOI: http://dx.doi.org/10.12989/sem.2016.57.3.441


# Wave propagation in functionally graded composite cylinders reinforced by aggregated carbon nanotube

Rasool Moradi-Dastjerdi*

*Young Researchers and Elite Club, Khomeinishahr Branch, Islamic Azad University, Khomeinishahr, Iran*

*(Received March 18, 2014, Revised December 28, 2015, Accepted January 11, 2016)*

**Abstract.** This work reports wave propagation in the nanocomposite cylinders that reinforced by straight single-walled carbon nanotubes based on a mesh-free method. Moving least square shape functions have been used for approximation of displacement field in weak form of motion equation. The straight carbon nanotubes (CNTs) are assumed to be oriented in specific or random directions or locally aggregated into some clusters. In this simulation, an axisymmetric model is used and also the volume fractions of the CNTs and clusters are assumed to be functionally graded along the thickness. So, material properties of the carbon nanotube reinforced composite cylinders are variable and estimated based on the Eshelby-Mori-Tanaka approach. The effects of orientation, aggregation and volume fractions of the functionally graded clusters and CNTs on dynamic behavior of nanocomposite cylinders are studied. This study results show that orientation and aggregation of CNTs have significant effects on the effective stiffness and dynamic behaviors.

**Keywords:** dynamic analysis; nanocomposite cylinder; aggregation; Eshelby-Mori-Tanaka; functionally graded; mesh-free

## 1. Introduction

Recently, the use of carbon nanotubes (CNTs) in polymer/carbon nanotube composites has attracted wide attention (Wagner *et al.* 1997). A high aspect ratio, low weight of CNTs and their extraordinary mechanical properties (strength and flexibility) provide the ultimate reinforcement for the next generation of extremely lightweight but highly elastic and very strong advanced composite materials. Most studies on nanocomposite reinforced by CNT have focused on their material properties (Griebel and Hamaekers 2004, Fidelus *et al.* 2005, Song and Youn 2006, Han and Elliott 2007, Zhu *et al.* 2007). Also some investigations like as Zhu *et al*. (2007), Manchado *et al*. (2005), Qian *et al*. (2000), Mokashi *et al*. (2007), have shown that the addition of small amount of CNT in the matrix can considerably improve the mechanical, electrical and thermal properties of polymeric composites.

One of the common features of CNT morphology is the formation of aggregation in the matrix. Aggregation into bundles or ropes limits the overall effectiveness of nanotubes at improving the

*Corresponding author, Ph.D., E-mail: rasoul.moradi@iaukhsh.ac.ir


http://www.techno-press.org/?journal=sem&subpage=8 ISSN: 1225-4568 (Print), 1598-6217 (Online)

mechanical properties of the nanocomposite. The large aspect ratio, nanotube volume fraction, low bending rigidity of CNTs and interfacial bonding in the inter-phase region between embedded CNT and its surrounding polymer lead to their aggregation. Local aggregation of the nanotube in the polymer host is reduced significantly by functionalizing the nanotubes, thereby increasing the compatibility with the polymer.

Montazeri *et al*. (2010) showed the influence of aggregation of nanotube using the modified Halpin-Tsi model. Also, they indicated above 1.5 wt.%, nanotubes agglomerate cases a reduction in Young's modulus values. Thus, it is important to determine the effect of the distribution and arrangement of CNTs on the effective properties of carbon nanotube reinforced composite (CNTRC). The Mori-Tanaka model is one of the best known analytical approaches to determine the effective material constants of composite materials. Barai and Weng (2011) developed a two-scale micromechanical model to analyze the effect of CNT aggregation and interface condition on the plastic strength of CNT/matrix inclusions, and the small scale addressed the property of the clustered inclusions. Yang *et al*. (2012) used the Mori-Tanaka approach to show the effect of CNT aggregation in the composite. They illustrated the degree of CNT aggregation dramatically influences the effective properties of the CNT/SMP composites. Tsai *et al*. (2011) used the Mori-Tanaka approach to show the effect of inclusion waviness and its distribution on the effective composite stiffness. They considered different waviness conditions: uniform waviness with variable inclusion orientation or aspect ratio, uniform aspect ratio and variable waviness and they understood that the inclusion waviness has a great effect on the tensile moduli and shear modulus for unidirectional composites. Shokrieh and Rafiee (2010a, b) studied the longitudinal behavior of a CNT in a polymeric matrix using a non-linear analysis on a full 3D multi-scale finite element model consisting of CNT, non-bonded inter phase region and surrounding polymer. The bonding between CNT and its surrounding polymer was simulated as Van der Waals interactions. Their finite element analysis results show that the rule of mixture for conventional composites overestimates the result and cannot capture the scale difference between micro- and nano-scale. However they developed an equivalent fiber to overcome this difficulty and corresponding longitudinal, transverse and shear moduli were calculated. Developed equivalent fiber consisting of CNT and inter-phase region can be appropriately used in micromechanical equations.

New class of materials known as functionally graded materials (FGMs) are special composites in which volume fractions of constituent materials vary uniformly and continuously along a certain direction(s). Therefore FGMs have a non uniform microstructure and a continuously variable macrostructure. By using the concept of FGM, Shen (2011) suggested that the interfacial bonding strength can be improved through the use of a graded distribution of CNTs in the matrix and investigated postbuckling of functionally graded nanocomposite cylindrical shells reinforced by SWCNTs subjected to axial compression in thermal environment and showed that the linear functionally graded reinforcements can increase the buckling load. The effects of waviness and aspect ratio of nanotube on the vibrational behavior of wavy CNT-reinforced cylinders were investigated by using a new version of rule of mixture to estimate of mechanical properties (Jam *et al*. 2012, Moradi-Dastjerdi *et al*. 2014). They considered different waviness conditions with variable aspect ratio and understood that the waviness has a significant effect on the natural frequency of nanocomposite cylindrical panels. Yas and Heshmati (2012) studied vibrational properties of FG-nanocomposite beams reinforced by randomly oriented straight SWCNTs under the action of moving load. They used the Eshelby-Mori-Tanaka approach based on an equivalent fiber to investigate the material properties of the beam and also they used FEM to discretize the model and obtain a numerical approximation of the motion equation. Sobhani Aragh *et al*. (2012)

presented vibrational behavior of continuously graded CNT-reinforced cylindrical panels based on the Eshelby-Mori-Tanaka approach. They used the 2-D Generalized Differential Quadrature Method (GDQM) to discretize the governing equations and to implement the boundary conditions.

For this study, a mesh-free method is used; MLS shape functions are used for approximation of displacement field in the weak form of motion equation. Static and dynamic analysis of FG-nanocomposite cylinders reinforced by straight SWCNTs carried out by the same mesh-free method that is used in this paper (Moradi-Dastjerdi *et al.* 2013a, b). But, effects of orientation and aggregation of straight CNTs were not considered in (Yas and Heshmati 2012, Sobhani Aragh *et al.* 2012, Moradi-Dastjerdi *et al.* 2013a, b). Also, Moradi-Dastjerdi *et al*. (2013c) presented axisymmetric natural frequencies of FG-CNTRC cylinders by the same mesh-free method and Eshelby-Mori-Tanaka approach in their study and showed these methods have very high accuracy for these problems. They assumed CNTs were oriented, aligned or randomly or locally aggregated into some clusters. Static, free vibration, dynamic and stress wave propagation analysis of isotropic FGM cylinders under an impact load were carried out by this mesh-free method (Foroutan *et al*. 2012, Mollarazi *et al*. 2011, Foroutan *et al*. 2011).

The main purpose of this study is investigation on the effects of orientation and aggregation of CNTs on radial displacement and stress wave propagations of functionally graded nanocomposite cylinders subjected to an impact load by the proposed mesh-free method. The CNTs are randomly oriented into some clusters. Volume fractions of the CNTs and clusters are assumed to be functionally graded in radial direction. Eshelbi-Mori-Tanaka approach has been proposed to explain the mechanical properties of the nanocomposites. This micromechanical model introduces a homogeneous composite. At first, based on the Eshelbi-Mori-Tanaka approach, effects of the orientation and aggregation of straight CNTs are investigated on the effective mechanical properties of nanocomposite. Then, except the effect of orientation and aggregation, effects of CNTs distribution kind in clusters and nanocomposite, CNTs volume fractions and cylinder thickness are investigated on the dynamic behavior of CNTRC cylinders.

## 2. Material properties in FG-CNT reinforced composite

Consider a CNTRC made from a mixture of SWCNT and matrix which is assumed to be isotropic. The SWCNT reinforcement is either uniformly distributed (UD) or functionally graded (FG) in the radial direction. Many studies have been published each with a different focus on mechanical properties of polymer nanotube composites. However, the common theme seems to have been enhancement of Young’s modulus. In this section, the effective mechanical properties of this composite are obtained based on the Eshelby-Mori-Tanaka approach. The CNTs were arranged within the matrix in such manner so as to introduce clustering. It has been observed that, due to large aspect ratio (usually >1000), low bending rigidity of CNTs and Van der Waals forces, CNTs have a tendency to bundle or cluster together making it quite difficult to produce fully-dispersed CNT reinforced composites. The effect of nanotube aggregation on the elastic properties of randomly oriented CNTRC is presented in this section. Shi *et al*. (2004) derived a two parameter micromechanics model to determine the effect of nanotube agglomeration on the elastic properties of randomly oriented CNTRC (Fig. 1). It is assumed that a number of CNTs are uniformly distributed throughout the matrix and the remained CNTs are aggregated in some cluster form, as shown in Fig. 1. The total volume of the CNTs in the representative volume element (RVE), denoted by $V_r$, can be divided into the following two parts

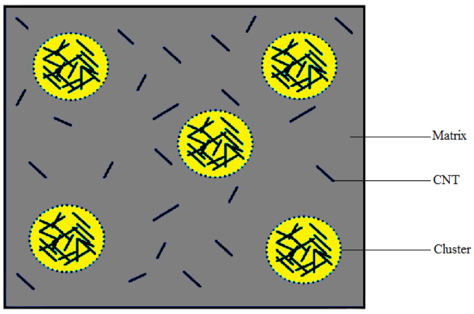


Fig. 1 RVE With Eshelby cluster model of aggregation of CNTs

$$V_r = V_r^{cluster} + V_r^m \tag{1}$$

where $V_r^{cluster}$ denotes the volume of CNTs inside a cluster, and $V_r^m$ is the volume of CNTs in the matrix and outside the clusters. The two parameters used to describe the aggregation are defined as

$$\mu = \frac{V_{cluster}}{V}\ ,\quad \eta = \frac{V_r^{cluster}}{V_r}\qquad 0 \le \eta, \mu \le 1 \tag{2}$$

where $V$ is volume of RVE, $V_{cluster}$ is volume of clusters in the RVE. $\mu$ is volume fraction of clusters with respect to the total volume $V$ of the RVE, $\eta$ is volume ratio of the CNTs inside the clusters over the total CNT inside the RVE. When $\mu$=1, this means uniform distribution of nanotubes throughout the entire composite without aggregation, and with the decreasing in $\mu$, the agglomeration degree of CNTs is more severe. When $\eta$=1, all the nanotubes are located in the clusters. The case $\eta=\mu$ means that the volume fraction of CNTs inside the clusters is as same as that of CNTs outside the clusters (fully-dispersed).

Thus, we consider the CNT-reinforced composite as a system consisting of clusters of sphere shape embedded in a matrix. We may first estimate respectively the effective elastic stiffness of the clusters and the matrix, and then calculate the overall property of the whole composite system. The effective bulk modulus, $K_{in}$, and shear modulus, $G_{in}$, of the cluster can be calculated by Prylutskyy *et al*. (2000), respectively

$$K_{in} = K_m + \frac{f_r \eta (\delta_r - 3K_m \alpha_r)}{3(\mu - f_r \eta + f_r \eta \alpha_r)} \tag{3}$$

$$G_{in} = G_m + \frac{f_r \eta (\eta_r - 2G_m \beta_r)}{2(\mu - f_r \eta + f_r \eta \beta_r)} \tag{4}$$

where

$$\alpha_r = \frac{3(K_m + G_m) + k_r - l_r}{3(G_m + k_r)} \tag{5}$$

$$\beta_r = \frac{1}{5}\left\{\frac{4G_m + 2k_r + l_r}{3(G_m + k_r)} + \frac{4G_m}{G_m + p_r} + \frac{2[G_m(3K_m + G_m) + G_m(3K_m + 7G_m)]}{G_m(3K_m + G_m) + m_r(3K_m + 7G_m)}\right\} \tag{6}$$

$$\delta_r = \frac{1}{3}\left[n_r + 2l_r + \frac{(2k_r + l_r)(3K_m + 2G_m - l_r)}{G_m + k_r}\right] \tag{7}$$

$$\eta_r = \frac{1}{5}\left[\frac{2}{3}(n_r - l_r) + \frac{8G_m p_r}{G_m + p_r} + \frac{8m_r G_m (3K_m + 4G_m)}{3K_m(m_r + G_m) + G_m(7m_r + G_m)} + \frac{2(k_r - l_r)(2G_m + l_r)}{3(G_m + k_r)}\right] \tag{8}$$

and the effective bulk modulus $K_{out}$ and shear modulus $G_{out}$ of the matrix outside the cluster can be calculated by (Shi *et al.* 2004)

$$K_{out} = K_m + \frac{f_r(1-\eta)(\delta_r - 3K_m\alpha_r)}{3[1-\mu - f_r(1-\eta) + f_r(1-\eta)\alpha_r]} \tag{9}$$

$$G_{out} = G_m + \frac{f_r(1-\eta)(\eta_r - 2G_m\beta_r)}{2[1-\mu - f_r(1-\eta) + f_r(1-\eta)\beta_r]} \tag{10}$$

$f_r$ and $f_m$ are the volume fractions for carbon nanotube and matrix. Finally, the effective bulk modulus $K$ and the effective shear modulus $G$ of the composite are derived from the Mori-Tanaka method as follows (Shi *et al.* 2004)

$$K = K_{out}\left[1 + \frac{\mu\left(\frac{K_{in}}{K_{out}} - 1\right)}{1 + \alpha(1-\mu)\left(\frac{K_{in}}{K_{out}} - 1\right)}\right] \tag{11}$$

$$G = G_{out}\left[1 + \frac{\mu\left(\frac{G_{in}}{G_{out}} - 1\right)}{1 + \beta(1-\mu)\left(\frac{G_{in}}{G_{out}} - 1\right)}\right] \tag{12}$$

with

$$\nu_{out} = \frac{(3K_{out} - 2G_{out})}{2(3K_{out} + G_{out})} \tag{13}$$

$$\alpha = \frac{(1+\nu_{out})}{3(1-\nu_{out})} \tag{14}$$

$$\beta = \frac{2(4-5\nu_{out})}{15(1-\nu_{out})} \tag{15}$$

The effective Young's modulus $E$ and Poisson's ratio $\upsilon$ of the composite in the terms of $K$ and $G$ are given by

$$E = \frac{9KG}{3K + G} \tag{16}$$

$$\upsilon = \frac{3K - 2G}{6K + 2G} \tag{17}$$

## 3. Governing equations

The weak form of motion equation in the absence of external forces is expressed by the following relation

$$\int_{\Omega} \boldsymbol{\sigma}.\delta(\boldsymbol{\varepsilon})dv - \int_{\Gamma} \mathbf{F}.\delta\mathbf{u}ds = -\int_{\Omega} \rho(r)\ddot{\mathbf{u}}.\delta\mathbf{u}dv \tag{18}$$

In the above relation, $\boldsymbol{\sigma}$, $\boldsymbol{\varepsilon}$, $\mathbf{F}$, $\mathbf{u}$ and $\ddot{\mathbf{u}}$ are stress, strain, surface traction, displacement and acceleration vectors respectively. $\boldsymbol{\Gamma}$ is a part of boundary of domain $\Omega$ on which traction $\mathbf{F}$ is applied. For axisymmetric problems stress and strain vectors are as follows

$$\boldsymbol{\sigma} = [\sigma_r, \sigma_\theta, \sigma_z, \sigma_{rz}]^T \quad , \quad \boldsymbol{\varepsilon} = [\varepsilon_r, \varepsilon_\theta, \varepsilon_z, \varepsilon_{rz}]^T \tag{19}$$

Stress vector is expressed in terms of strain vector by means of Hook's law

$$\boldsymbol{\sigma} = \mathbf{D}\boldsymbol{\varepsilon} \tag{20}$$

Matrix $\mathbf{D}$ is defined in Foroutan and Moradi-Dastjerdi (2011) for an isotropic cylinder.

## 4. Mesh-free numerical analysis

In these analyses moving least square (MLS) shape functions introduced by Lancaster and Salkauskas (1981) is used for approximation of displacement vector in the weak form of motion equation. Displacement vector $\mathbf{u}$ can be approximated by MLS shape functions as follows

$$\mathbf{u} = [u_r, u_z]^T = \boldsymbol{\Phi}\hat{\mathbf{u}} \tag{21}$$

where $\hat{\mathbf{u}}$ and $\boldsymbol{\Phi}$ are virtual nodal values vector and shape functions matrix respectively.

$$\hat{\mathbf{u}} = [(\hat{u}_r)_1, (\hat{u}_z)_1, \ldots\ldots\ldots.(\hat{u}_r)_n, (\hat{u}_z)_n]^T \tag{22}$$

and

$$\boldsymbol{\Phi} = \begin{bmatrix} \Phi_1 & 0 & \Phi_2 & 0 & . & . & . & . & \Phi_n & 0 \\ 0 & \Phi_1 & 0 & \Phi_2 & . & . & . & . & 0 & \Phi_n \end{bmatrix} \tag{23}$$

By using Eq. (21) for approximation of displacement vector, strain vector can be expressed in terms of virtual nodal values

$$\boldsymbol{\varepsilon} = \mathbf{B}\hat{\mathbf{u}} \tag{24}$$

where matrix $\mathbf{B}$ is defined as follows

$$\mathbf{B} = \begin{bmatrix} \frac{\partial\Phi_1}{\partial r} & 0 & \frac{\partial\Phi_2}{\partial r} & 0 & . & .. & . & . & \frac{\partial\Phi_n}{\partial r} & 0 \\ \frac{\Phi_1}{r} & 0 & \frac{\Phi_2}{r} & 0 & . & .. & . & . & \frac{\Phi_n}{r} & 0 \\ 0 & \frac{\partial\Phi_1}{\partial z} & 0 & \frac{\partial\Phi_2}{\partial z} & . & .. & . & . & 0 & \frac{\partial\Phi_n}{\partial z} \\ \frac{\partial\Phi_1}{\partial z} & \frac{\partial\Phi_1}{\partial r} & \frac{\partial\Phi_2}{\partial z} & \frac{\partial\Phi_2}{\partial r} & . & .. & . & . & \frac{\partial\Phi_n}{\partial z} & \frac{\partial\Phi_n}{\partial r} \end{bmatrix} \tag{25}$$

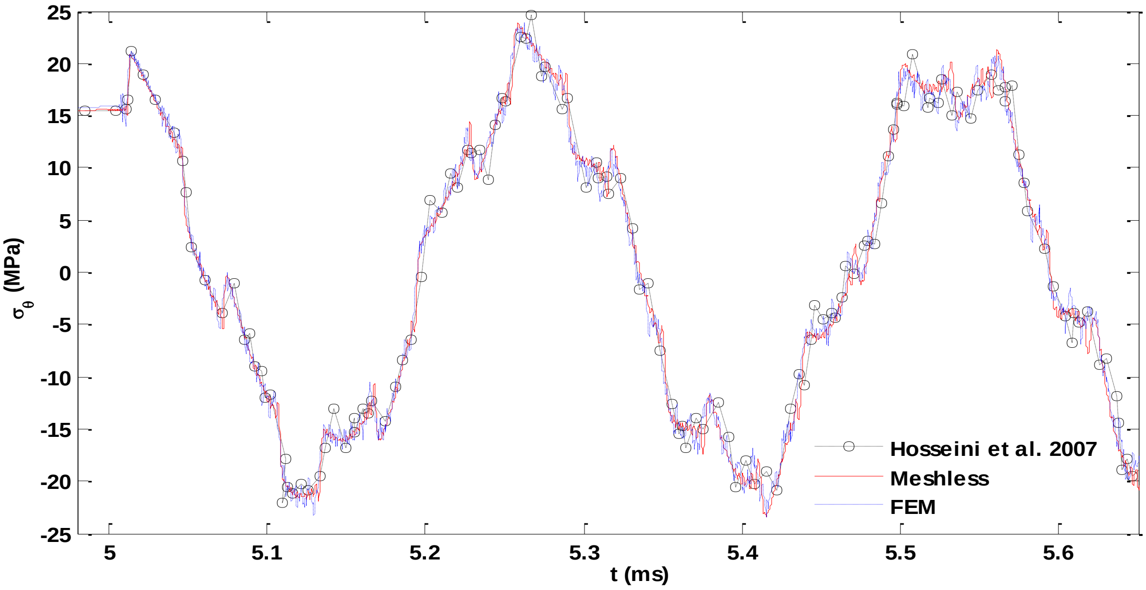


Fig. 2 Time history of hoop stress at midpoint of FGM cylinder with *n*=0.5

Substitution of Eqs. (20)-(21) and (24) in Eq. (18) leads to

$$\mathbf{M}\ddot{\hat{\mathbf{u}}} + \mathbf{k}\hat{\mathbf{u}} = \mathbf{f} \tag{26}$$

where

$$\mathbf{M} = \int_{\Omega} \rho \mathbf{\Phi}^T \mathbf{\Phi} dv \qquad \mathbf{k} = \int_{\Omega} \mathbf{B}^T \mathbf{D} \mathbf{B} dv \qquad \mathbf{f} = \int_{\Gamma} \mathbf{\Phi}^T \mathbf{F} ds \tag{27}$$

For numerical integration, problem domain is discretized to a set of background cells with gauss points inside each cell. Then global stiffness matrix **k** is obtained numerically by sweeping all gauss points inside $\mathbf{\Omega}$. Similarly global force vector **f** is formed numerically in the same manner but by sweeping all gauss points on $\mathbf{\Gamma}$.

## 5. Results and discussions

Stress wave propagations and radial displacements of these CNTRC cylinders are determined by solving motion Eq. (26), based on the Newmark (central difference) method. Eq. (26) is derived by discretizing of the domain in suitable node arrangements. For deriving and solving of Eq. (26), a computer code is developed in MATLAB environment.

At first step of this section, the proposed mesh-free method and the model calculations of the nanocomposite modulus are validated. Then the effects of orientation and aggregation of the CNTs located in the matrix on the mechanical properties of these cylinders are investigated. After all, effects of various parameters on the dynamic behaviors of CNTRC cylinders are investigated.

### *5.1 Validation of models*

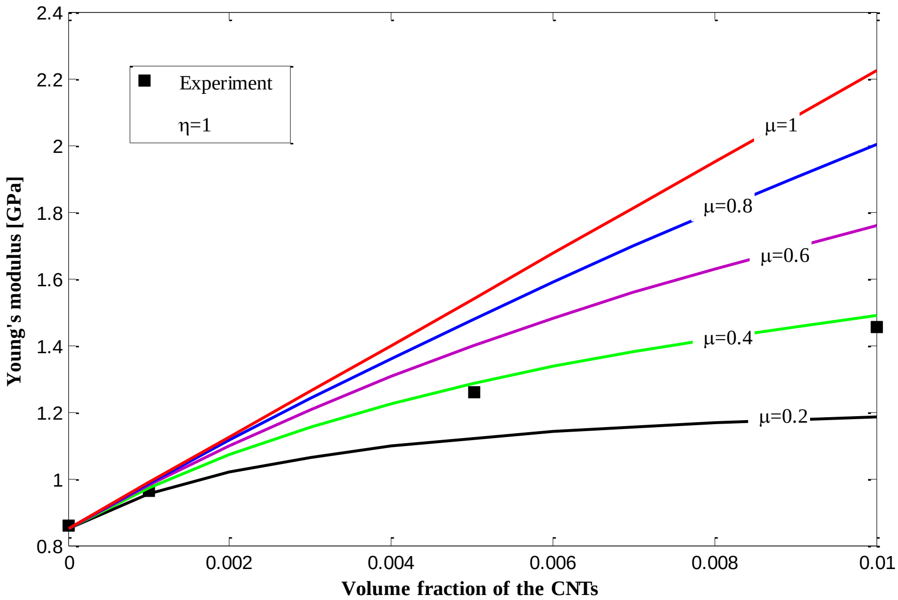


Fig. 3 Comparison of the Young's modulus of CNT-reinforced composite at different degree of aggregation with the experimental data (Odegard *et al*. 2003)

For validation of the proposed mesh-free method (as Moradi-Dastjerdi *et al.* 2013b), an FGM cylinder in plane strain state subjected to a shock loading is considered like as Hosseini *et al.* (2007). Variation of mechanical properties along the radius is as follows

$$p = p_i + \left(\frac{r - r_i}{r_o - r_i}\right)^n (p_o - p_i) \tag{28}$$

where, $p_i$ and $p_o$ are mechanical properties at inner and outer surfaces respectively with $n$=0.5. By solving system of differential Eq. (26) for this cylinder, displacement field is obtained as a function of time. Time history of hoop stress at midpoint of cylinder is shown in Fig. 2. In this figure, results obtained from the proposed mesh-free method are compared with both FEM results and results reported by Hosseini *et al*. (2007). This comparison shows a good agreement between them.

After validation of proposed mesh-free model, the Mori-Tanaka approach that is applied for calculation of the nanocomposite modulus is examined. This approach can determine the effects of orientation and aggregation of the CNTs in the matrix. These cases have a significant effect on the material properties of CNT nanocomposite. As mentioned before, $\mu$ and $\eta$ are respectively indicators of the volume fraction of clusters and CNTs in the clusters. Fig. 3 shows Young's modulus of a CNT-reinforced composite for different values of $\mu$ when $\eta$=1, that are compared with the experimental data (Odegard *et al.* 2003). This figure shows that fully dispersion of randomly oriented CNTs ($\mu$=1) has the biggest value of Young's modulus. Also, decreasing of $\mu$ in constant value of $\eta$ and CNTs volume fraction (increasing of CNTs aggregation) decreases the Young's modulus. It can be seen that the experimental data and the aggregation state of $\eta$=1 and $\mu$=0.4 are nearly the same. These results are in agreement with an argument proposed by Barai and

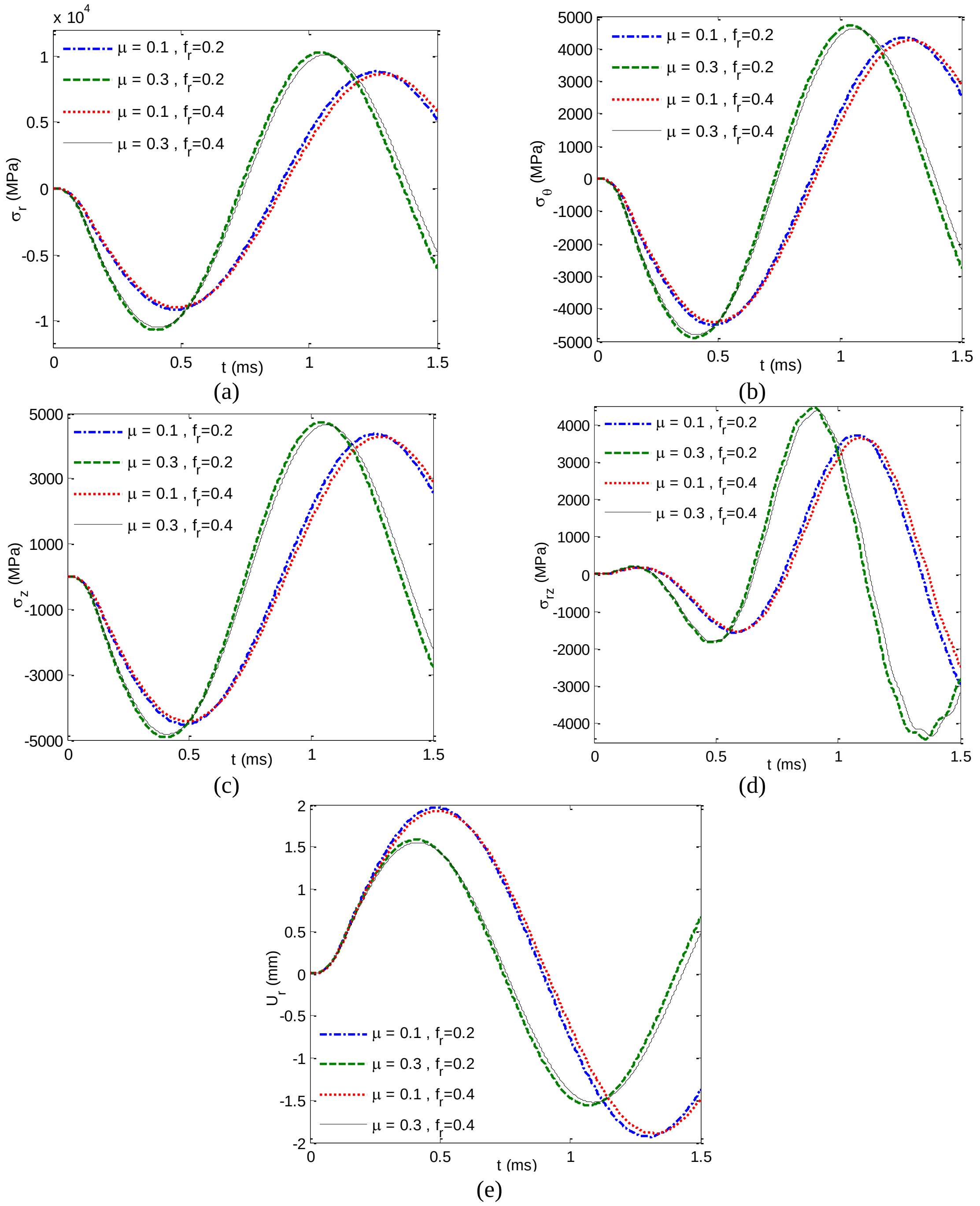


Fig. 4 Time history of (a) Radial stress, (b) hoop stress, (c) axial stress, (d) shear stress and (e) radial displacement at mid radius of the CNTRC cylinders with $r_i$=0.4, $r_o$=0.5 and $\eta$=1

Weng (2011). Moradi-Dastjerdi *et al*. (2013c) reported that fully dispersion of the randomly oriented CNTs, $\mu$=$\eta$, has maximum value of Young's modulus also, increasing of $\eta$ (for constant

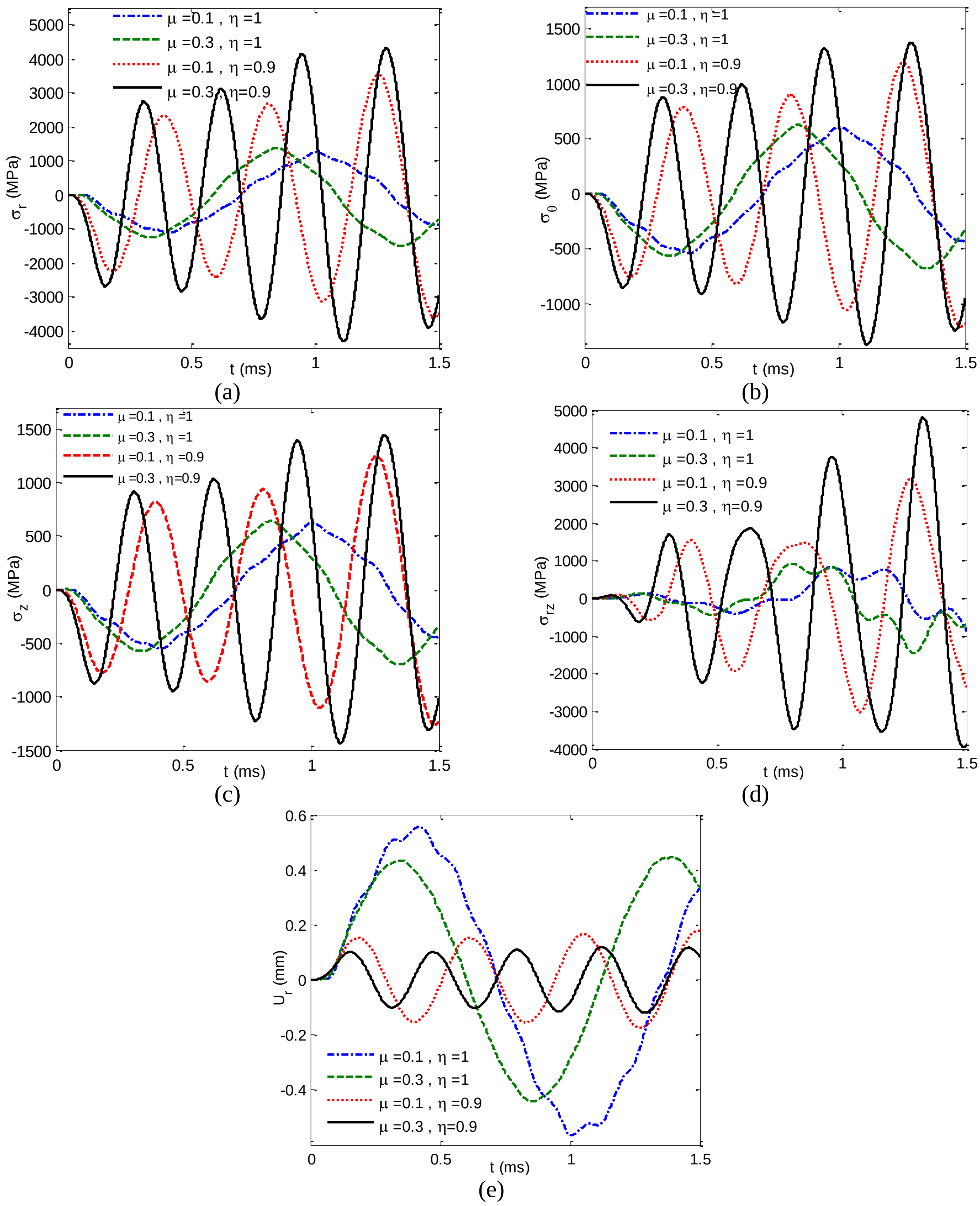


Fig. 5 Time history of (a) Radial stress, (b) hoop stress, (c) axial stress, (d) shear stress and (e) radial displacement at mid radius of the CNTRC cylinders with $r_i$=0.25, $r_o$=0.5 and $f_r$=0.2

$\mu$) and decreasing of $\mu$ (for constant $\eta$) lead to decreasing of effective Young's modulus of the composite.

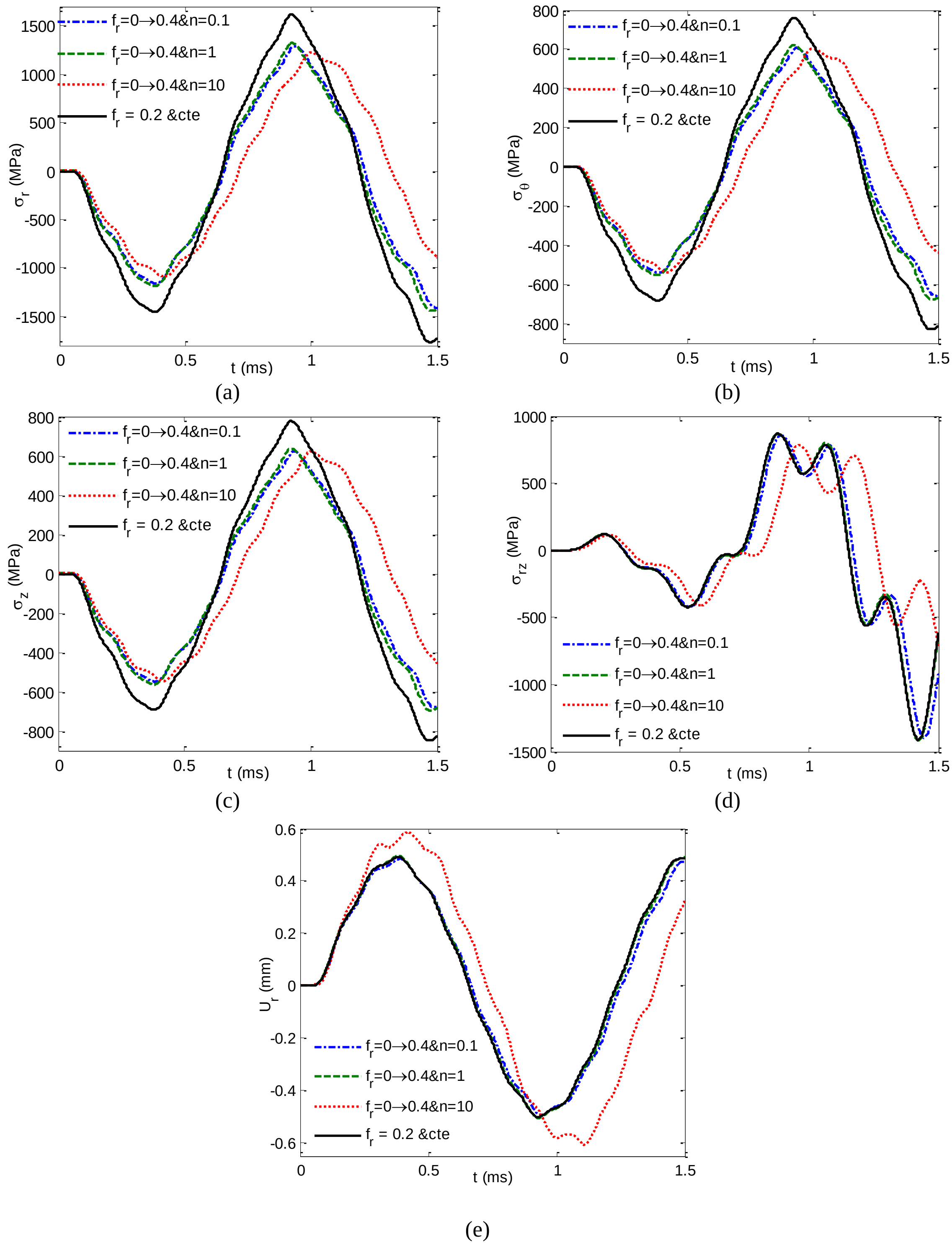


Fig. 6 Time history of (a) Radial stress, (b) hoop stress, (c) axial stress, (d) shear stress and (e) radial displacement at mid radius of the CNTRC cylinders with $r_i$=0.25, $r_o$=0.5, $\mu$=0.2 and $\eta$=1

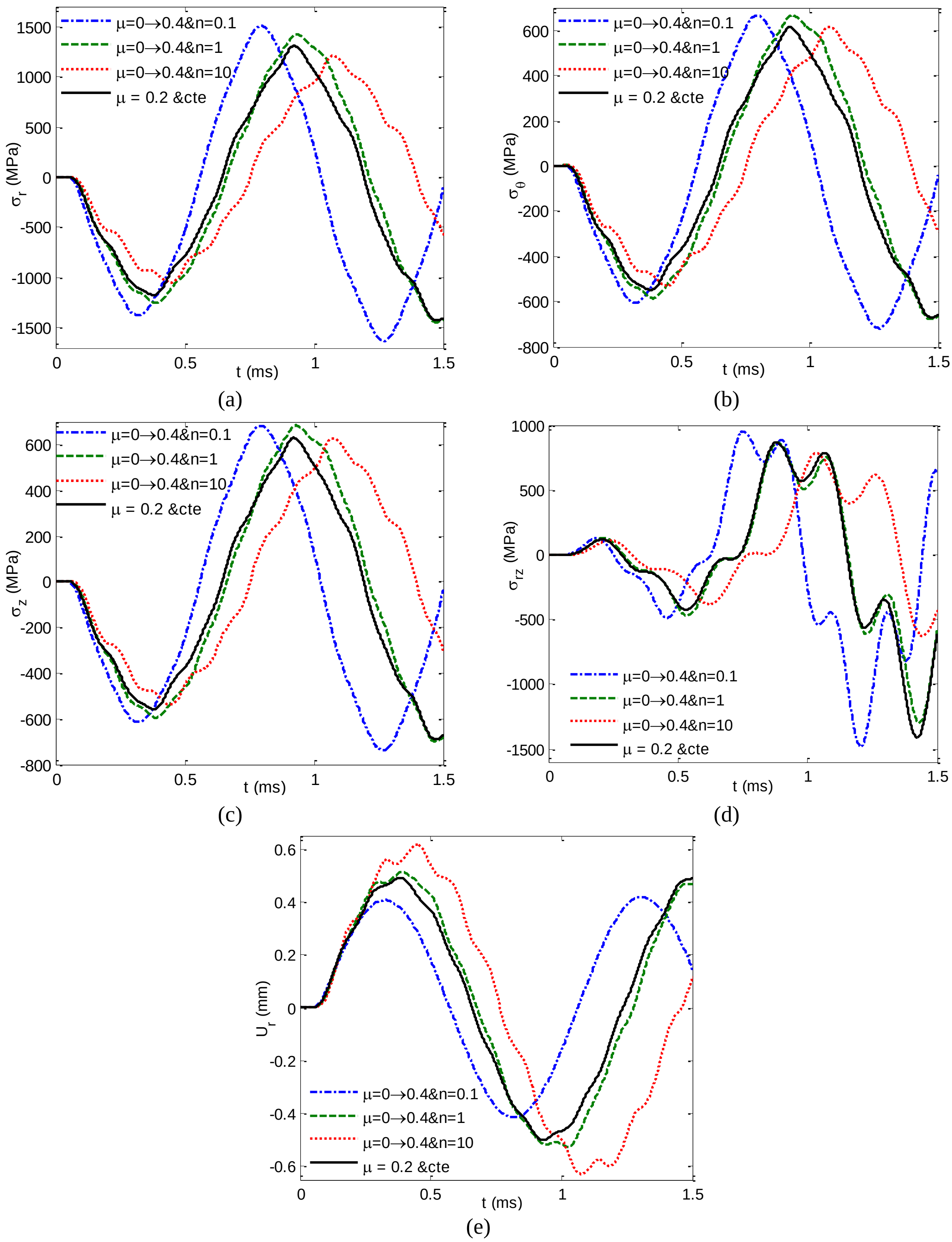


Fig. 7 Time history of (a) Radial stress, (b) hoop stress, (c) axial stress, (d) shear stress and (e) radial displacement at mid radius of the CNTRC cylinders with $r_i$=0.25, $r_o$=0.5, $f_r$=0.2 and $\eta$=1

### 5.2 Wave propagation analysis of CNTRC cylinders

After validation of the proposed methods, various models of hollow CNRTC cylinders are analyzed for investigation of effects of cylinder thickness, CNTs volume fractions, $f_r$, clusters volume fractions, $\mu$, CNTs inside the clusters, $\eta$, and volume fraction powers, *n*, on $f_r$ and $\mu$. These hollow CNTRC cylinders are in plane strain state and subjected to an impact load as an internal pressure expressed by

$$\begin{aligned} &P(t)=P_0 \sin\left(\frac{\pi t}{0.00015}\right) \quad \text{for } t \le 0.00015 \text{ (s)} \\ &P(t)=0 \qquad\qquad\qquad\quad \text{for } t > 0.00015 \text{ (s)} \end{aligned} \tag{29}$$

where $P_0$=10 MPa. In the following simulations, CNTRC cylinders are considered made of Poly (methyl-methacrylate, referred as PMMA) as matrix, with CNT as fibers. PMMA is an isotropic material with $E^m$=2.5 GPa, $\rho^m$=1150 Kg/m$^3$ and $\upsilon^m$=0.34. The (10, 10) SWCNTs are selected as reinforcements. The adopted material properties for SWCNT are: $E_1^{CN}=5.6466\,TPa$, $E_2^{CN}=7.0800\,TPa$, $G_{12}^{CN}=1.9445\,TPa$, $\rho^{CN}$=1400 Kg/m$^3$ and $\upsilon^{CN}$=0.175 (Shen 2011).

At first, infinite length CNTRC cylinders are considered with internal radius of $r_i$=0.4 m and external radius of $r_o$=0.5 m. In these cylinders, all of the CNTs are located in clusters, $\eta$=1. Fig. 4 show time history of radial, hoop, axial and shear stresses and also radial displacement at mid radius (*r*=0.45 m) for different values of clusters volume, $\mu$, and CNTs volume, $f_r$. It can be seen, due to increasing of the Young's modulus of CNTRC, increasing of the cluster volumes increases speed and amplitude of the stress wave propagation also, increases speed, but decreases amplitude of the radial displacements. These figures reveal that increasing in the CNTs volume fractions leads to decrease in speed and amplitude of stress wave propagations. It's considerable that, unlike CNT volume fraction, cluster volume has significant effect on the dynamic behavior. Also, radial, hoop and axial stress wave propagations have almost same styles of variation while the radial stresses have their biggest values. At second, effect of the cylinder thickness is examined. So, consider previous CNTRC cylinders with constant CNTs volume fractions, $f_r$=0.2, internal radius of $r_i$=0.25 m and external radius of $r_o$=0.5 m. Fig. 5 illustrate stress wave propagations and radial displacement of these cylinders for various aggregation states (different values of the $\mu$ and $\eta$). These figures show that decreasing of $\eta$ or increasing of $\mu$, increase speed and amplitude in stress wave propagations while variation of the $\eta$ has a significant effect on the wave speed due to increasing of the stiffness of CNTRC (Moradi-Dastjerdi *et al.* 2013c). Comparing Fig. 5 with Fig. 4 reveals that decreasing the cylinder thickness increases values of stresses and radial displacement considerably. In FG-CNTRC cylinders, a property of nanocomposite such as volume fraction of nanotube, $f_r$, or clusters, $\mu$, varies along the radius according to Eq. (28). At third models, consider UD and FG-CNTRC cylinders with aggregation state of $\mu$=0.2 and $\eta$=1. In these cylinders, volume fraction of nanotube, $f_r$, varies from zero to 0.4, according to Eq. (28). Fig. 6 shows waves propagations of these FG-CNTRC cylinders for different values of volume fraction powers, *n*, that are compared by results of an UD-CNTRC cylinder with $f_r$=0.2. It can be seen that increasing of *n* (due to decreasing CNTs volume fractions) from 0.1 to 1, doesn't have significant effect on the dynamic behavior. But in *n*=10, volume fraction of CNTs decreases dramatically, so the speed of wave propagation decreases considerably. Finally, the effect of FG modes in clusters is investigated. Consider CNTRC cylinders with $f_r$=0.2, $\eta$=1 and previous dimension. In these cylinders, volume of clusters, μ, varies from zero to 0.4 according to Eq. (28). Fig. 7 show dynamic responses of the FG cylinders that are compared by dynamic responses of a cylinder with constant volume of clusters equal to, $\mu$=0.2. It's observed, increasing of *n*, decreases waves speed considerably, but decreases their amplitudes a little. Also, in the same clusters volume fraction, linear FG mode of clusters (*n*=1) has closed dynamic behavior with UD mode.

## 6. Conclusions

The effects of orientation and aggregation of CNTs on the wave propagation of functionally graded nanocomposite cylinders reinforced by straight carbon nanotube were analyzed numerically based on a mesh-free method. Volume fractions of CNTs and clusters were assumed to be functionally graded along the thickness, so that material properties of CNTRC cylinders were variable and estimated based on the Eshelby-Mori-Tanaka approach. It is observed that those kinds of distributions and aggregation of CNTs had significant effects on the effective stiffness and wave propagation. Also, effects of CNTs volume fractions and cylinder thickness were investigated and also the following results were obtained:

- Increasing of the CNTs volume fractions decreases speed and amplitude of stress wave propagation.
- Unlike CNT volume fraction, cluster volume has significant effect on the dynamic behavior.
- Increasing of the CNT volume fraction power (*n*) decreases speed and amplitude of wave propagation.
- Increasing of the clusters volume fraction powers (*n*) considerably decreases waves speed but it has a little decreases in amplitude.
- In the same clusters volume fraction, linear FG mode of clusters (*n*=1) has closed dynamic behavior with UD mode.
- Decreasing of the cylinder thickness increases values of the stresses and radial displacement considerably.

## References

Barai, P. and Weng, G.J. (2011), “A theory of plasticity for carbon nanotube reinforced composite”, *Int. J. Plast*., **27**, 539-59.

Fidelus, J.D., Wiesel, E., Gojny, F.H., Schulte, K. and Wagner, H.D. (2005), “Thermo-mechanical properties of randomly oriented carbon/epoxy nanocomposites”, *Compos. Part A*, **36**, 1555-61.

Foroutan, M. and Moradi-Dastjerdi, R. (2011), “Dynamic analysis of functionally graded material cylinders under an impact load by a mesh-free method”, *Acta Mech.*, **219**, 281-90.

Foroutan, M., Moradi-Dastjerdi, R. and Sotoodeh-Bahreini, R. (2012), “Static analysis of FGM cylinders by a mesh-free method”, *Steel Compos. Struct.*, **12**, 1-12.

Griebel, M. and Hamaekers, J. (2004), “molecular dynamic simulations of the elastic moduli of polymer-carbon nanotube composites”, *Comput. Meth. Appl. Mech. Eng*., **193**, 1773-88.

Han, Y. and Elliott, J. (2007), “Molecular dynamics simulations of the elastic properties of polymer/carbon nanotube composites”, *Comput. Mater. Sci.*, **39**, 315-23.

Hosseini, S.M., Akhlaghi, M. and Shakeri, M. (2007), “Dynamic response and radial wave propagation velocity in thick hollow cylinder made of functionally graded materials”, *Int. J. Comput. Aid. Eng. Softw.*, **24**, 288-303.

Jam, J.E., Pourasghar, A. and Kamarian, S. (2012), “The effect of the aspect ratio and waviness of CNTs on the vibrational behavior of functionally graded nanocomposite cylindrical panels”, *Polym. Compos.*, **33**,

2036-44.
Lancaster, P. and Salkauskas, K. (1981), "Surface generated by moving least squares methods", *Math. Comput.*, **37**, 141-58.
Manchado, M.A.L., Valentini, L., Biagiotti, J. and Kenny, J.M. (2005), "Thermal and mechanical properties of single-walled carbon nanotubes-polypropylene composites prepared by melt processing", *Carbon*, **43**, 1499-505.
Mokashi, V.V., Qian, D. and Liu, Y.J. (2007), "A study on the tensile response and fracture in carbon nanotube-based composites using molecular mechanics", *Compos. Sci. Technol*., **67**, 530-40.
Mollarazi, H.R., Foroutan, M. and Moradi-Dastjerdi, R. (2011), "Analysis of free vibration of functionally graded material (FGM) cylinders by a meshless method", *J. Compos. Mater.*, **46**, 507-15.
Montazeri, A., Javadpour, J., Khavandi, A., Tcharkhtchi, A. and Mohajeri, A. (2010), "Mechanical properties of multi-walled carbon nanotube/epoxy composites", *Mater. Des*., **31**, 4202-8.
Moradi-Dastjerdi, R., Pourasghar, A., Foroutan, M. and Bidram, M. (2014), "Vibration analysis of functionally graded nanocomposite cylinders reinforced by wavy carbon nanotube based on mesh-free method", *J. Compos. Mater.*, **48**, 1901-13.
Moradi-Dastjerdi, R., Foroutan, M. and Pourasghar, A. (2013), "Dynamic analysis of functionally graded nanocomposite cylinders reinforced by carbon nanotube by a mesh-free method", *Mater. Des.*, **44**, 256-66.
Moradi-Dastjerdi, R., Foroutan, M., Pourasghar, A. and Sotoudeh-Bahreini, R. (2013), "Static analysis of functionally graded carbon nanotube-reinforced composite cylinders by a mesh-free method", *J. Reinf. Plast. Compos.*, **32**, 593-601.
Moradi-Dastjerdi, R., Pourasghar, A. and Foroutan, M. (2013), "The effects of carbon nanotube orientation and aggregation on vibrational behavior of functionally graded nanocomposite cylinders by a mesh-free method", *Acta Mech.*, **224**, 2817-32.
Odegard, G.M., Gates, T.S., Wise, K.E., Park, C. and Siochi, E.J. (2003), "Constitutive modeling of nanotube-reinforced polymer composites", *Compos. Sci. Technol*., **63**, 1671-1687.
Prylutskyy, Y.I., Durov, S.S., Ogloblya, O.V., Buzaneva, E.V. and Scharff, P. (2000), "Molecular dynamics simulation of mechanical, vibrational and electronic properties of carbon nanotubes", *Comput. Mater. Sci.*, **17**, 352-355.
Qian, D., Dickey, E.C., Andrews, R. and Rantell, T. (2000), "Load transfer and deformation mechanisms in carbon nanotube-polystyrene composites", *Appl. Phys. Lett.*, **76**, 2868-70.
Shen, H.S. (2011), "Postbuckling of nanotube-reinforced composite cylindrical shells in thermal environments, Part I: Axially-loaded shells", *Compos. Struct.*, **93**, 2096-108.
Shi, D.L., Feng, X.Q., Yonggang, Y.H., Hwang, K.C. and Gao, H. (2004), "The effect of nanotube waviness and agglomeration on the elasticproperty of carbon nanotube reinforced composites", *J. Eng. Mater. Technol*., **126**, 250-257.
Shokrieh, M. and Roham, R. (2010), "Prediction of mechanical properties of an embedded carbon nanotube in polymer matrix based on developing an equivalent long fiber", *Mech. Res. Commun*., **37**, 235-40.
Shokrieh, M. and Roham, R. (2010), "On the tensile behavior of an embedded carbon nanotube in polymer matrix with non-bonded interphase region", *Compos. Struct*., **92**, 647-52.
Sobhani Aragh, B., Nasrollah Barati, A.H. and Hedayati, H. (2012), "Eshelby-Mori-Tanaka approach for vibrational behavior of continuously graded carbon nanotube-reinforced cylindrical panels", *Compos. Part B*, **43**, 1943-54.
Song, Y.S. and Youn, J.R. (2006), "Modeling of effective elastic properties for polymer based carbon nanotube composites", *Polym.*, **47**, 1741-8.
Tsai, C., Zhang, C., Jack, D.A., Liang, R. and Wang, B. (2011), "The effect of inclusion waviness and waviness distribution on elastic properties of fiber-reinforced composites", *Compos. Part B*, **42**, 62-70.
Wagner, H.D., Lourie, O., Feldman, Y. and Tenne, R. (1997), "Stress-induced fragmentation of multiwall carbon nanotubes in a polymer matrix", *Appl. Phys. Lett.*, **72**, 188-90.
Yang, Q.S., He, X.Q., Liu, X., Leng, F.F. and Mai, Y.W. (2012), "The effective properties and local aggregation effect of CNT/SMP composites", *Compos. Part B*, **43**, 33-8.

Yas, M.H. and Heshmati, M. (2012), "Dynamic analysis of functionally graded nanocomposite beams reinforced by randomly oriented carbon nanotube under the action of moving load", *Appl. Math. Model*., **36**, 1371-94.

Zhu, R., Pan, E. and Roy, A.K. (2007), "Molecular dynamics study of the stress-strain behavior of carbon-nanotube reinforced Epon 862 composites", *Mater. Sci. Eng. A*, **447**, 51-7.

*CC*